The Astrophysical Journal, 668:826–838, 2007 October 20

THE HIERARCHICAL BUILD-UP OF MASSIVE GALAXIES AND THE INTRACLUSTER LIGHT SINCE $z = 1$

Charlie Conroy,[1] Risa H. Wechsler,[2] and Andrey V. Kravtsov[3]

Received 2007 March 14; accepted 2007 July 6

ABSTRACT

We use a set of simulation-based models for the dissipationless evolution of galaxies since $z = 1$ to constrain the fate of accreted satellites embedded in dark matter subhalos. These models assign stellar mass to dark matter halos at $z = 1$ by relating the observed galaxy stellar mass function (GSMF) to the halo + subhalo mass function monotonically. The evolution of the stellar mass content is then followed using halo merger trees extracted from *N*-body simulations. Our models are differentiated only in the fate assigned to satellite galaxies once subhalos, within which satellites are embedded, disrupt. These models are confronted with the observed evolution in the massive end of the GSMF, the $z \sim 0$ brightest cluster galaxy (BCG) to cluster mass relation, and the combined BCG and intracluster light (ICL) luminosity distribution—all observables expected to evolve approximately dissipationlessly since $z = 1$. The combined observational constraints favor a model in which the vast majority ($\gtrsim 80\%$) of satellite stars from disrupted subhalos go into the ICL (operationally defined here as light below a surface brightness cut of $\mu_i \approx 23$ mag arcsec^{-2}). Conversely, models that leave behind a significant population of satellite galaxies once the subhalo has disrupted are strongly disfavored, as are models that put a significant fraction of satellite stars into the BCG. Our results show that observations of the ICL provide useful and unique constraints on models of galaxy merging and the dissipationless evolution of galaxies in groups and clusters.

Subject headings: cosmology: theory — dark matter — galaxies: clusters: general — galaxies: evolution — galaxies: halos — galaxies: luminosity function, mass function

Online material: color figures

1. INTRODUCTION

The formation and evolution of massive ($M_{\rm star} \gtrsim 10^{11}\ M_\odot$) elliptical galaxies is thought to be inexorably linked to the formation and evolution of the large-scale structure of the universe. The classical picture wherein massive elliptical galaxies form "monolithically" at $z > 5$ (Partridge & Peebles 1967) has been replaced by more nuanced scenarios that decouple the epoch at which these galaxies formed the bulk of their stars from the epoch (or epochs) at which these stars were assembled to form the final galaxy. These more complex scenarios arise fairly naturally within the context of the hierarchical growth of structure in the now favored ΛCDM cosmology (see, e.g., Baugh et al. 1996; Neistein et al. 2006). While stellar population modeling has firmly placed the epoch of star formation in these galaxies at $z > 2$ (e.g., Bower et al. 1992; Trager et al. 2000; van Dokkum & Franx 2001; Thomas et al. 2005; Jimenez et al. 2006), the assembly history of massive galaxies is still far from clear, and is the focus of this work.

The evolving space density of massive galaxies over time provides important clues to their assembly history. Evolution in the galaxy stellar mass function (GSMF) since $z \sim 1$ appears quite mild for the most massive galaxies (Fontana et al. 2004, 2006; Drory et al. 2004; Bundy et al. 2005; Borch et al. 2006; Cimatti et al. 2006; Andreon 2006). Estimates of evolution in the luminosity function are also more or less consistent with massive galaxies passively evolving from $z \approx 1$ to the present (Cirasuolo et al. 2006; Wake et al. 2006; Faber et al. 2005; Willmer et al. 2006; Brown et al. 2007; Caputi et al. 2006; Blanton 2006). These same observations also find roughly a doubling in the *total* stellar mass density from $z \sim 1$ to $z \sim 0$—the implication being that star formation occurs primarily in less massive galaxies at $z < 1$. In addition to number counts, estimates of the merger rate of massive galaxies can in principle constrain their assembly history, although current observations fail to present a consistent picture (e.g., van Dokkum 2005; Bell et al. 2006; Masjedi et al. 2006). Finally, it has been suggested that dissipationless galaxy-galaxy mergers may play an important role in determining the structural properties of massive elliptical galaxies (Naab et al. 2006).

The majority of massive elliptical galaxies are (or have been in their recent past) the brightest cluster galaxies within large group- or cluster-sized halos (referred to simply as "clusters" in the remainder of the paper), located near the centers of the halo potential well. It is thus interesting to study the formation of such galaxies in the general context of cluster formation. If, as recent observations suggest, the majority of massive galaxies were already in place at $z \sim 1$, then on the surface it appears difficult to reconcile this with the much more substantial evolution of their host dark matter halos (massive halos grow by factors of $\gtrsim 3$ in mass since $z = 1$). It is one of the goals of the present work to address and resolve this tension.

Within the ΛCDM framework, groups and clusters of galaxies are expected to be continually accreting new galaxies. After entering a cluster, the stars in satellite galaxies can (1) be all deposited onto the central galaxy, (2) stay bound as a satellite galaxy, or (3) be scattered into the intracluster light (ICL). For the purposes of this study we define the ICL as the stars beyond the optical radius of the central galaxy, i.e., the light not accounted for in the photometry of the central galaxy itself. In reality, a combination of these possibilities can occur. For example, a satellite galaxy can

[1] Department of Astrophysical Sciences, Peyton Hall, Princeton University, Princeton, NJ 08544.

[2] Kavli Institute for Particle Astrophysics and Cosmology, Physics Department, and Stanford Linear Accelerator Center, Stanford University, Stanford, CA 94305.

[3] Department of Astronomy and Astrophysics, Kavli Institute for Cosmological Physics; and The Enrico Fermi Institute, The University of Chicago, 5640 S. Ellis Avenue, Chicago, IL 60637.

be partially stripped and deposit a fraction of its stellar mass into the ICL before merging and contributing the rest of the stars to the central galaxy. In addition, when two massive galaxies merge, a certain fraction of stars will acquire large kinetic energy and will move to large radii, outside the optical radius of the remnant. While evolution in the space density of massive galaxies strongly constrains the importance of the first scenario, this observation cannot readily distinguish between scenarios two and three.

Fortunately, fates (2) and (3) have effects on observable properties of the ICL, which can thus constrain the amount of stars that can be lost to the ICL during mergers or tidal stripping. These observations suggest that the fraction of total cluster light bound up in the ICL is ∼10%–30% (Zibetti et al. 2005; Gonzalez et al. 2005; Krick et al. 2006), with the ICL comprising a significant fraction (∼50%–80%) of the combined light from the central galaxy and ICL (Gonzalez et al. 2005; Seigar et al. 2007 note that this fraction depends sensitively on the way that the ICL and BCG are separated). In addition, models in which the stellar component of satellite halos is never disrupted by tides would have quite different predictions for the number of satellite galaxies in a halo of a given mass, and thus for the small-scale clustering of galaxies (see, e.g., Berlind & Weinberg 2002). Indeed, the clustering of massive galaxies in combination with their evolving space density has recently been exploited by White et al. (2007) to constrain the disruption rate of massive satellite galaxies between $z \simeq 0.9$ and $z \simeq 0.5$.

The goal of this study is to confront these and other observational constraints *simultaneously* with a series of simple, simulation-based models in order to gain insight into the fate(s) of satellite stars. The models presented herein combine a simple prescription for relating galaxies to dark matter halos at $z \sim 1$ with the assembly history of these halos extracted from *N*-body simulations in order to follow the dissipationless growth of massive galaxies to $z \sim 0$. The relation between galaxies and halos at $z \sim 1$ is generated by assigning the most massive galaxies to the most massive halos monotonically. This has been shown to successfully reproduce a wide variety of observations (Colín et al. 1999; Kravtsov & Klypin 1999; Neyrinck et al. 2004; Kravtsov et al. 2004; Vale & Ostriker 2004, 2006, 2007; Tasitsiomi et al. 2004; Conroy et al. 2006; Shankar et al. 2006). Note that this model considers both subhalos, which are halos contained within the virial radii larger halos, and what we will call distinct halos, which are halos not contained within the virial radii of larger halos. We follow the dynamical evolution of subhalos after they accrete onto their host halo using merger trees extracted directly from cosmological simulations, rather than a semianalytic model.

Semianalytic models (SAMs) for the formation and evolution of galaxies within a cosmological context, depending on the adopted assumptions about galaxy formation physics, are capable of predicting both strong (Baugh et al. 1996; De Lucia et al. 2006) and mild (Bower et al. 2006; Kitzbichler & White 2007; Monaco et al. 2006) evolution in the number density of massive galaxies since $z \sim 1$. The most massive galaxies in many of these models have formed the bulk of their stars at $z > 2$, in agreement with observations. Hence differences between these models are due primarily to different treatments of the assembly history of the massive galaxies.

Our approach is similar in spirit to that of a recent study by Monaco et al. (2006), who used the MORGANA SAM (Monaco et al. 2007) to follow the evolution of galaxies. These authors artificially turned off star formation at $z < 1$ in order to follow the dissipationless growth of galaxies at late times, similar to what we do here. The orbital evolution of satellites in their SAM was computed with simple analytical approximations to dynamical friction, tidal heading, and tidal stripping. Monaco et al. (2006) showed that the observed evolution in the space density of massive galaxies is reproduced in their model only if they allow for >30% of stars from disrupted satellites to be transferred into the ICL. The present work goes further than the study of Monaco et al. (2006) by (1) using an independent set of simulations with satellite tracks extracted directly from the simulations and (2) comparing to a wider array of observations and hence providing more general constraints on the fates of the stars within satellite galaxies.

The rest of this article unfolds as follows. In § 2 we describe the simulations, halos catalogs and merger trees used in this analysis. § 3 outlines the details of our models and § 4 contains comparisons between the models and several observations. The implications of these results and comparison to related work is discussed in § 5. Throughout this paper we assume a ΛCDM cosmology with $(\Omega_m, \Omega_\Lambda, h, \sigma_8) = (0.3, 0.7, 0.7, 0.9)$, except in § 2 where we leave quantities in terms of the reduced Hubble constant, h.

2. SIMULATIONS, HALO CATALOGS, AND MERGER TREES

The simulations used here were run with the Adaptive Refinement Tree (ART) *N*-body code (Kravtsov et al. 1997; Kravtsov 1999). The ART code implements successive refinements in both the spatial grid and temporal step in high-density environments. These simulations were run in the concordance flat ΛCDM cosmology with $\Omega_m = 0.3 = 1 - \Omega_\Lambda$, $h = 0.7$, where Ω_m and Ω_Λ are the present-day matter and vacuum densities in units of the critical density, and h is the Hubble parameter in units of 100 km s^{-1} Mpc^{-1}. The power spectra used to generate the initial conditions for the simulations were determined from a direct Boltzmann code calculation (courtesy of Wayne Hu). We use a power spectrum normalization of $\sigma_8 = 0.90$, where σ_8 is the rms fluctuation in spheres of 8 h^{-1} Mpc comoving radius.

The simulation used herein was run in a box of length 120 h^{-1} Mpc with particle mass $m_p = 1.07 \times 10^9\ h^{-1}\ M_\odot$, peak force resolution of $h_{\rm peak} = 1.8\ h^{-1}$ kpc, and 512^3 particles. We have checked that our results remain unchanged when utilizing a smaller box with smaller particle mass (a box of length 80 h^{-1} Mpc with particle mass $m_p = 3.16 \times 10^8\ h^{-1}\ M_\odot$).

From this simulation we generate dark matter halo catalogs and dark matter halo merger trees. Our models rely not only on distinct halos, i.e., halos with centers that do not lie within any larger virialized system, but also subhalos, which are located with the virial radii of larger systems. When we refer to a "halo" generically we mean both distinct halos and subhalos.

Distinct halos and subhalos are identified using a variant of the bound density maxima (BDM) halo finding algorithm (Klypin et al. 1999). Details of the algorithm and parameters used can be found in Kravtsov et al. (2004); we briefly summarize the main steps here. All particles are assigned a density using the `smooth` algorithm[4] which uses a symmetric SPH smoothing kernel on the 32 nearest neighbors. Starting with the highest overdensity particle, we surround each potential center by a sphere of radius $r_{\rm find} = 50\ h^{-1}$ kpc and exclude all particles within this sphere from further search. Hence no two halos can be separated by less than $r_{\rm find}$. We then construct density, circular velocity, and velocity dispersion profiles around each center, iteratively removing unbound particles as described in Klypin et al. (1999). Once unbound particles have been removed, we measure quantities such as $V_{\rm max} = \left[GM(<r)/r\right]^{1/2}\big|_{\rm max}$, the maximum circular velocity of the halo. For each distinct halo we calculate the virial radius, defined as

[4] To calculate the density we use the publicly available code smooth: http://www-hpcc.astro.washington.edu/tools/tools.html.

the radius enclosing overdensity of 334 with respect to the *mean* density of the universe at the epoch of the output. We use this virial radius to classify objects into distinct halos and subhalos. The halo catalogs are complete for halos with more than 50 particles, which corresponds, for the box with length 120 h^{-1} Mpc, to $5.35 \times 10^{10}\ h^{-1}\ M_{\odot}$.

Halo merger trees have also been constructed for this simulation (for a detailed description of the merger tree construction, see Allgood 2005). These merger trees allow us to tabulate $M_{\rm vir}^{\rm acc}$ for subhalos, the virial mass at the time when a subhalo first crosses the virial radius of a distinct halo. Since subhalos are subject to dynamical processes such as tidal stripping, $M_{\rm vir}^{\rm acc}$ will always be greater than or equal to the present $M_{\rm vir}$. This accretion epoch quantity is used in our models, to which we now turn.

3. THE MODELS

3.1. *Connecting Galaxies to Halos*

Recent studies have shown that models in which galaxies are associated with the centers of dark matter halos and subhalos accurately reproduce a wide variety of observations both at low and high redshift (e.g., Kravtsov et al. 2004; Vale & Ostriker 2004; Conroy et al. 2006). Herein, stellar mass is assigned to each halo in a simulation by assuming a monotonic relation between stellar mass and halo virial mass using the observed GSMF and halo mass function measured in simulations:

$$n_g(>M_{{\rm star},i}) = n_h(>M_{{\rm vir},i}), \tag{1}$$

where n_g and n_h are the number density of galaxies and halos (note again that "halos" here and throughout refers to both distinct halos and their subhalos), respectively. Galaxy stellar masses can hence be assigned to halos at any epoch once the GSMF at that epoch is known. In the simplest version of this scheme there is assumed to be no scatter in the relation between halo mass and stellar mass (see § 4.5 for a discussion of scatter in the context of our models).

Subhalos lose mass due to tidal stripping as they orbit within their parent halo. Since stripping primarily affects the outer regions of the subhalo, we expect the galaxy, which resides within the inner few kpc of the subhalo, to be relatively unaffected by this process. Hence, for subhalos, when relating halo mass to luminosity or stellar mass we use its virial mass at the epoch when it is first accreted onto the parent halo, $M_{\rm vir}^{\rm acc}$, rather than its mass at the epoch of observation. This choice is well motivated both by hydrodynamical simulations (Nagai & Kravtsov 2005) and detailed modeling of the small to intermediate scale ($0.1 < r < 10\ h^{-1}$ Mpc) clustering of galaxies over a range of redshifts (Conroy et al. 2006).

One may ask to what extent it is justifiable to identify satellite galaxies with subhalos in dissipationless simulations. It has been shown that the subhalo population in dissipationless simulations is indeed quite similar to the galaxy population in hydrodynamical simulations (Zheng et al. 2005; Weinberg et al. 2006) and semianalytic models (Zheng et al. 2005). In particular, satellite populations in these hydrodynamical simulations with cooling and galaxy formation have an almost identical halo occupation distribution to the subhalos in dissipationless simulations. These conclusions are corroborated by the general success of the subhalo-based models of galaxy clustering.

This model, for example, accurately captures observed relations between cluster luminosity and the number of galaxies within a cluster as a function of cluster mass (Vale & Ostriker 2004, 2006), the luminosity dependence of the galaxy-matter cross-correlation function (after a reasonable amount of scatter is introduced into this relation; see Tasitsiomi et al. 2004 for details), close pair counts (Berrier et al. 2006), the luminosity, scale, and redshift dependence of the galaxy autocorrelation function from $z \sim 5$ to $z \sim 0$ (Conroy et al. 2006), and mass-to-light ratios in local clusters (Tasitsiomi et al. 2007).

Emboldened by the success of this simple model, in the present work we extend it by populating halos with galaxies at $z \sim 1$ in the above way and then using halo merger trees derived from N-body simulations to follow the evolution of these galaxies to $z \sim 0$. Specifically, we use the observed GSMF of Fontana et al. (2006) at $z \sim 1$ to assign stellar masses to halos, and then follow the *dissipationless* evolution of these galaxies via the merging history of their dark matter halos to $z \sim 0$. This exercise is appropriate for the evolution of the most massive galaxies, as these galaxies formed the bulk of their stars at $z > 2$ (e.g., Bower et al. 1992; Trager et al. 2000; van Dokkum & Franx 2001; Thomas et al. 2005; Jimenez et al. 2006) and hence largely evolve dissipationlessly at $z < 1$. Note that neglecting star formation at $z < 1$ means that the evolution of the total stellar mass predicted by our models is a lower limit on the actual evolution.

The following $z = 1$ GSMF Schechter parameters are adopted from Fontana et al. (2006):

$$\begin{aligned} \alpha &= -1.26 \pm 0.1, \\ M_* &= 10^{11.01 \pm 0.1}\ M_{\odot}, \\ \phi_* &= (7.6 \pm 2.4) \times 10^{-4}\ {\rm Mpc}^{-3}. \end{aligned} \tag{2}$$

The 1 σ errors quoted above are not the statistical errors reported in Fontana et al. (2006) but are instead meant to roughly encompass the various published estimates of the $z = 1$ GSMF Schechter parameters. The statistical errors are a factor of 2–3 smaller than these approximate systematic errors. Here and throughout the Chabrier initial mass function (IMF) is used when quoting stellar masses.

It is important to note that while different authors derive somewhat different Schechter parameters for the $z \sim 1$ GSMF, all authors agree that the massive end of the GSMF ($>M_*$) evolves very little, if at all, since $z \sim 1$. In addition, while several measurements of the GSMF at $z \sim 1$ have relied on photometric redshifts (e.g., Borch et al. 2006), the general conclusions from these studies have been supported by measurements which utilize spectroscopic redshifts (Bundy et al. 2006; Fontana et al. 2006).

Figure 1 presents a comparison between various observed GSMFs at $z \sim 1$ and the $z \sim 0$ GSMF from Cole et al. (2001). Note that the $z \sim 1$ GSMF used in our models (Fontana et al. 2006) is below all the other $z \sim 1$ GSMFs. This implies that our results concerning the $z = 0$ brightest cluster galaxy (BCG) luminosities derived with this GSMF will be lower bounds relative to the other GSMFs.

At $z = 1$, a space density of $10^{-4}\ {\rm Mpc}^{-3}$ corresponds to halos of virial mass $M_{\rm vir} \sim 4 \times 10^{13}\ M_{\odot}$ and stellar mass $M_{\rm star} \sim 3 \times 10^{11}\ M_{\odot}$. At this space density, ~17% of halos are subhalos at $z \sim 0$. Finally, note that although we formally assign stellar mass to all the halos found in the simulations and track their evolution as described in the following section, our results are quite insensitive to low-mass halos and are instead governed by the evolution and fate of much more massive halos. Since it is these halos that are most easily resolved and tracked from time step to time step, we expect our results to be insensitive to our simulation resolution.

3.2. *Dynamical Evolution Models*

Our model contains (at least) three adjustable components. The first is our assumed cosmology and will be fixed throughout,

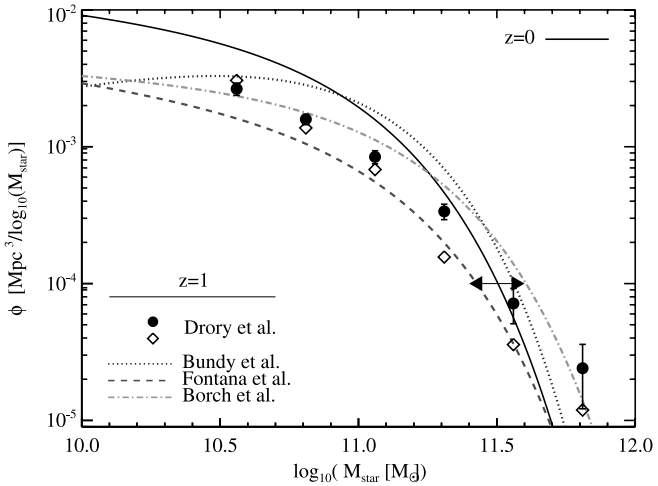

FIG. 1.—Observed GSMFs. The nonsolid lines are best-fit Schechter functions to the following GSMFs at $z \sim 1$: Borch et al. (2006; *dot-dashed line*), Bundy et al. (2006; *dotted line*), and Fontana et al. (2006; *dashed line*). The GSMF from Drory et al. (2004) is plotted directly, both for their fiducial GSMF (*diamonds*) and an estimate that includes lost-light corrections (*filled circles;* error bars are Poisson uncertainties only). The GSMF at $z \sim 0$ from Cole et al. (2001; *solid line*) is also included, along with arrows indicating a change of 0.2 dex in $M_{\rm star}$ at $\phi = 10^{-4}$. [*See the electronic edition of the Journal for a color version of this figure.*]

although we comment qualitatively on the effects of changing certain cosmological parameters in § 4.5. The second component is our input method for assigning stellar masses to halos at $z \sim 1$. In § 4.5 we demonstrate that our results are robust to reasonable changes of this second component. In particular, we introduce scatter in the assignment between stellar mass and halo mass and marginalize over the uncertainties in the $z \sim 1$ GSMF and find no qualitative change to our conclusions, provided that the true GSMF is not considerably different from recent estimates.

The third adjustable component is the most uncertain and concerns how we treat subhalos that have dropped out of the halo catalog. This can occur either because the subhalo is physically disrupted or because it is stripped below the resolution limit of the simulation; it is often quite difficult to distinguish these two cases within the simulation. We do nothing to the galaxies assigned to subhalos while the subhalos remain identifiable in our simulation—i.e., the satellite galaxy within the subhalo experiences no tidal stripping. Once a subhalo is destroyed, we are free to redistribute the stars from this subhalo in one or more of the ways outlined in the Introduction. To summarize that discussion: the stars can be deposited onto the central galaxy (this assumes that the satellite within the destroyed subhalo has merged with the central galaxy), can remain as a satellite galaxy without an identifiable subhalo, and/or the stars can be added to the intracluster light (ICL). In the latter case the stars are added to the outer regions of the central galaxy, beyond the optical radius (the radius within which the central galaxy luminosity is measured).

In order to explore these possibilities, four models are constructed that differ only in the fate of the stars within disrupted subhalos. Model Sat2Cen assumes that all of the stars are deposited onto the central galaxy. Conversely, model KeepSat assumes that the stars remain bound as a satellite galaxy. Model Sat2ICL assumes that all stars are deposited into the ICL. Finally, model Sat2Cen+ICL assumes that the stars are distributed equally between the ICL and the central galaxy. We will assume below, when comparing to observations of the ICL, that the ICL in these models is generated predominantly from the remnants of mergers with the central galaxy at $z < 1$. These assumptions are motivated by hydrodynamical simulations of clusters (Willman et al. 2004; Murante et al. 2004; Rudick et al. 2006; Murante et al. 2007; Sommer-Larsen et al. 2005) that showed that the majority of the ICL is built up at $z < 1$ from major mergers with the central galaxy, rather than tidal stripping as the satellite orbits in the cluster. For reference, these models are summarized in Table 1.

These models have implicitly assumed that all stellar mass at $z = 1$ persists to $z = 0$. However, stellar mass loss due to winds and supernovae can result in a significant decrease in the aggregate stellar mass of a population over time. In order to understand these effects, consider a secular mass-loss rate of $\dot{M}/M = 0.05\ (t/{\rm Gyr})^{-1}$ for a stellar population formed in an instantaneous burst and older than a few hundred Myr (Jungwiert et al. 2001). If massive red galaxies grew most of their stellar mass in the form of a single burst at $z = 2$, then the fraction of stellar mass lost between $z = 1$ and $z = 0$ is only 7%; however, if the stars in these galaxies all formed at $z = 1$ then the fraction is 36%. Since observations place the epoch of star formation in these massive galaxies at $z \gtrsim 2$, mass-loss effects are likely unimportant.

3.3. *Generating Luminosities*

Comparison to observations in §§ 4.2 and 4.3 will require conversion from stellar masses to *K*-band and *I*-band luminosities, respectively. To make this conversion we use the relation between mass-to-light ratios and colors provided by Bell et al. (2003),

$$\begin{aligned} M_{\rm star}/L_K &= 0.72, \\ M_{\rm star}/L_I &= 1.90, \end{aligned} \tag{3}$$

where we have assumed a color of $(u - r) = 2.5$ and $(B - R) = 1.5$ when deriving $M_{\rm star}/L_K$ and $M_{\rm star}/L_I$, respectively, and a Chabrier IMF. These colors are appropriate for the bright end of the red sequence (Pahre 1999; Baldry et al. 2004; Bell et al. 2003). The scatter in M/L is $\sim$0.1 dex for the bright red galaxies that will be the focus of this paper and can be attributed primarily to variations in metallicity. The possible effects of including the observed scatter in M/L will be implicitly explored in § 4.5.2.

All the results to be discussed below are independent of our assumed IMF because we are only interested in relative evolution from $z = 1$ to $z = 0$. Thus, so long as the observations at these epochs use the same IMF, the results are insensitive to the particular IMF used (whether for example Chabrier, Kroupa, or Salpeter IMFs are used). Results which concern luminosities are also IMF independent so long as we use a mass-to-light ratio with the same IMF as used in our GSMFs (as we have done above).

TABLE 1
SUMMARY OF MODELS

Model	Fate of Satellite Galaxy in a Disrupted Subhalo
Sat2Cen	Stars deposited onto the central galaxy
KeepSat	Stars remain bound as a satellite galaxy
Sat2ICL	Stars deposited into the ICL
Sat2Cen+ICL	Stars divided equally between the ICL and the central galaxy

The luminosities of galaxies at $z \sim 0$ in these models are strictly lower bounds for two reasons: (1) these models neglect star formation since $z = 1$, and (2) some galaxies might not be as red as the colors assumed in the previous paragraph, and hence they will be brighter at a fixed stellar mass. For the massive BCGs studied herein, however, these effects are unimportant. It will become apparent in the next section that including these possibilities would only strengthen our general conclusions since both residual star formation and bluer colors would increase the BCG luminosities and the evolution of the massive end of the GSMF.

We also assume that the ICL has the same color as the tip of the red sequence when converting ICL stellar mass to luminosities. Such an assumption appears borne out by observations of an at most weak color gradient out to several hundred kpc from the BCG, with some authors finding a slight reddening (Gonzalez et al. 2000; Krick et al. 2006) and others a slightly bluer color, or no gradient at all (Zibetti et al. 2005).

4. RESULTS

We now compare the models constructed in § 3 to the observed evolution in the galaxy stellar mass function (§ 4.1), to the relation between BCG luminosity and cluster virial mass at $z \sim 0$ (§ 4.2), and to properties of the intracluster light (ICL; § 4.3). In § 4.4 we discuss these models in the context of star formation since $z = 1$; at the end of this section several caveats and assumptions made herein are explored.

4.1. *Evolution in the GSMF*

In this section we present the evolution in the galaxy stellar mass function (GSMF) for the models described in § 3, and compare to observations. An effective way to quantify the evolution in the massive end of the GSMF is by quantifying the change of stellar mass corresponding to galaxies with a fixed given value of spatial number density. Hence, we define the quantity M_{-4}, such that $\phi(M_{-4}) = 10^{-4}$, and its evolution as $\Delta M_{-4} \equiv \log_{10}(M_{-4}^{z=0}) - \log_{10}(M_{-4}^{z=1})$ (for a pictorial representation, Fig. 2, *top panel*). This quantity is more stable than its inverse (the evolution in the number density of a given stellar mass) due to the exponential cutoff of the GSMF at high stellar masses. Note that M_{-4} is dominated by the space density of massive, rare objects.

Uncertainties in the observed $z \sim 1$ GSMF are incorporated into the models by generating 200 realizations of the GSMF with each Schechter parameter drawn from a Gaussian distribution with mean and dispersion equal to the best fit and 1 σ errors on the observed GSMF (see eq. [2]). We have tried other GSMFs at $z \sim 1$ (Bundy et al. 2006; Borch et al. 2006) and find qualitatively similar results.

The bottom panel of Figure 2 shows the distribution of ΔM_{-4} generated from the 200 Monte Carlo realizations for models Sat2Cen and Sat2Cen+ICL (models KeepSat and Sat2ICL produce no/little change in ΔM_{-4}, see below). A rough observational limit of 0.2 dex is denoted by the shaded band and has been estimated from observations of the $z = 1$ GSMF (see Fig. 1). As can be seen from Figure 1, this limit is probably an upper bound because several GSMFs at $z \sim 1$ are actually above the $z \sim 0$ GSMF, which is in all likelihood unphysical and is likely attributable to a combination of cosmic variance and photometric redshift uncertainties. Future observations will be needed to quantify in more detail the evolution of the massive end of the GSMF since $z = 1$.

For each model the predicted evolution in ΔM_{-4} is a lower bound since star formation between $z \sim 1$ and $z \sim 0$, which is neglected in these models, will increase ΔM_{-4}. However, since the massive galaxies which dominate this quantity have formed

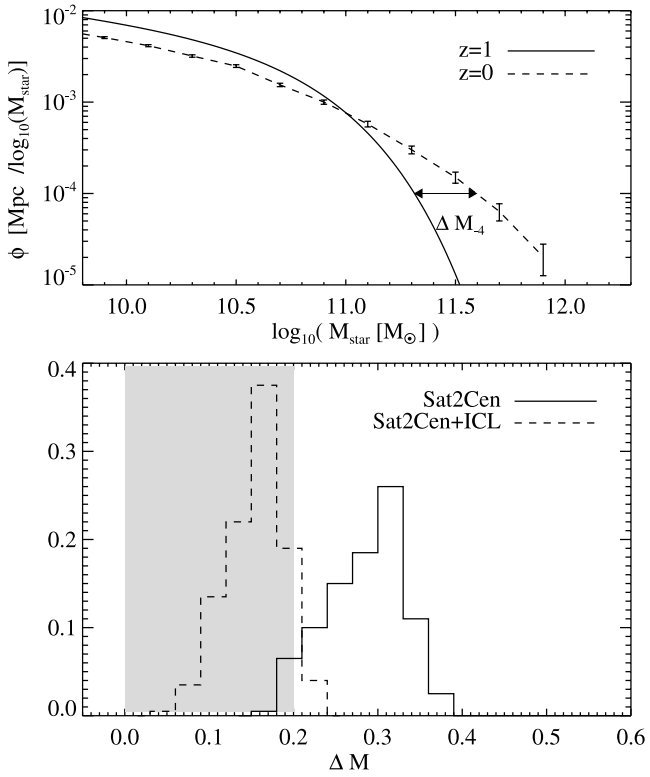

FIG. 2.—Evolution in the GSMF from $z \sim 1$ to $z \sim 0$. *Top panel:* Pictorial representation of how we quantify evolution in the massive end of the GSMF with the parameter ΔM_{-4}, for one realization of model Sat2Cen (error bars denote Poisson uncertainty only). See the text for details. *Bottom panel:* Distributions of ΔM_{-4} for models Sat2Cen and Sat2Cen+ICL. These distributions are obtained by running each model using a slightly different GSMF to populate halos at $z \sim 1$. Model KeepSat predicts no change in the entire GSMF and hence $\Delta M_{-4} \equiv 0$ for that model, while model Sat2ICL results in $\Delta M_{-4} \sim 0$. Running models for a series of GSMFs demonstrates the effect of uncertainties in the $z \sim 1$ GSMF on our results. Observational limits are denoted by the shaded region. [*See the electronic edition of the Journal for a color version of this figure.*]

the bulk of their stars at $z > 1$, we expect the contribution to ΔM_{-4} from star formation to be unimportant. Note that the evolution in the GSMF presented in Figure 2 makes no reference to the observed $z \sim 0$ GSMF. We simply compare the observed GSMF at $z = 1$ with the GSMF evolved to $z = 0$ with our models. For comparison, $\Delta M_{-4} = 0.4$ for dark matter halos in our adopted cosmology.

For each model, the differences in ΔM_{-4} for different $z \sim 1$ GSMF Schechter parameters arise because different Schechter parameters result in a different relation between stellar mass and dark matter halo mass, via equation (1). The growth of a dark matter halo and, through our models, the growth of the central galaxy, is driven by accreted halos spanning a range in mass. Therefore, the predicted growth of the central galaxy mass will change, if the mapping between halo mass and stellar mass changes. We now explain the behavior of each model in turn.

Model Sat2Cen displays the largest increase in M_{-4} because massive galaxies, which by definition dominate this quantity, are growing rapidly. In this model, galaxies with $M_{\rm star} > 10^{11}\ M_{\odot}$ at $z = 0$ have on average more than doubled in mass since $z = 1$. Rapid growth of massive galaxies occurs in this case because the satellite galaxies within disrupted subhalos add all of their stars onto the central massive galaxy. Model KeepSat predicts $\Delta M_{-4} \equiv 0$, since in this model galaxies do not evolve, i.e., galaxies neither merge nor form stars since $z = 1$. In Model Sat2ICL the massive end of the GSMF does not increase (but in some realizations

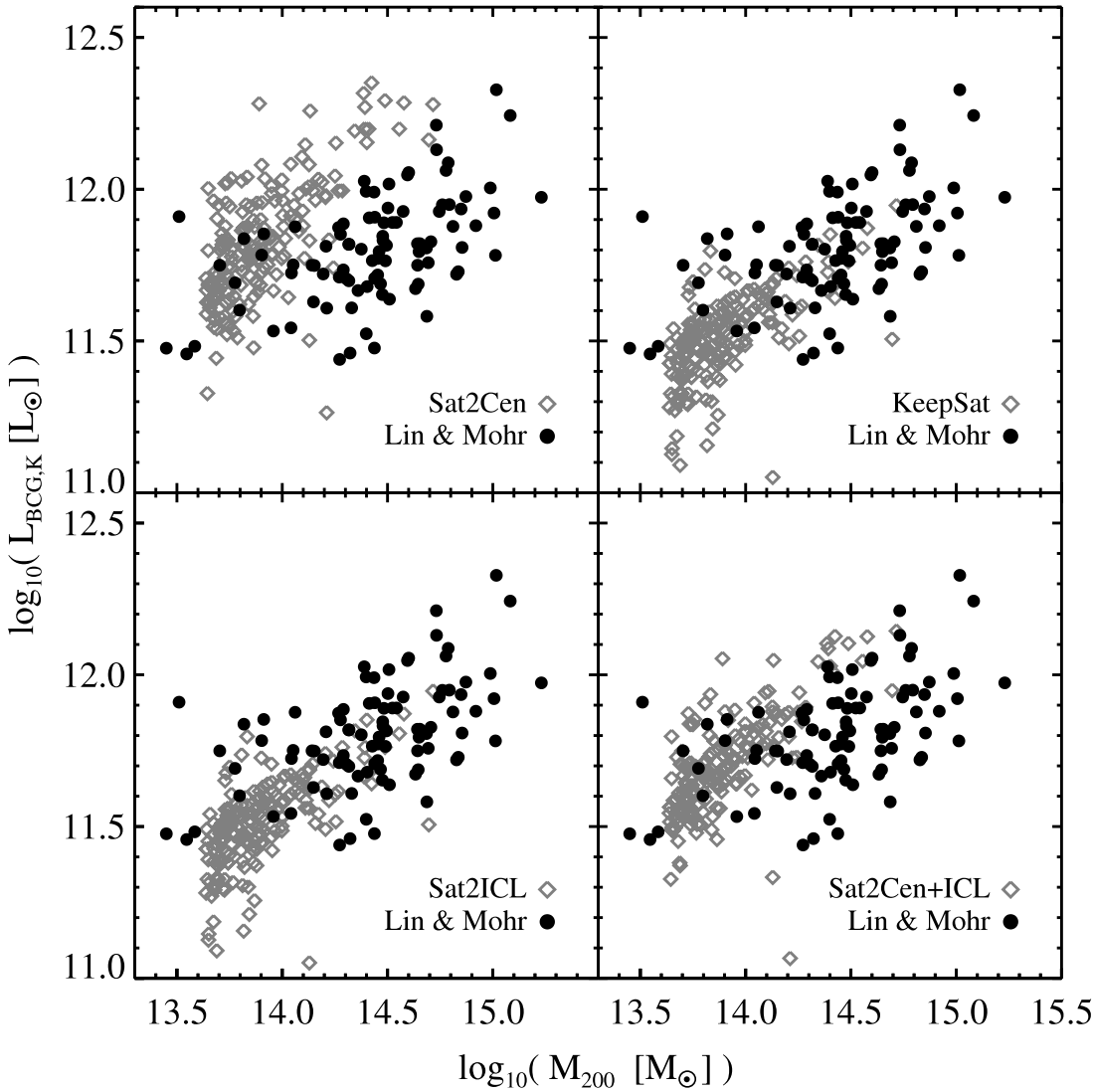

FIG. 3.—Luminosity of the BCG as a function of the cluster virial mass, comparing data from Lin & Mohr (2004; *filled circles*) to models (*open diamonds*). [*See the electronic edition of the Journal for a color version of this figure*.]

actually decreases slightly with time as some very massive satellite galaxies disrupt) because the stars within satellite galaxies are transferred to the ICL, which, for the purposes of the GSMF amounts to deleting the galaxy from the sample. Model Sat2Cen+ICL is, by construction, intermediate between models Sat2Cen and Sat2ICL, since half of the stars from disrupted subhalos are deposited onto the central galaxy and the rest into the ICL. In this model the most massive galaxies have increased in mass by the more modest factor of $\sim$50% since $z = 1$.

Based on the evolution in the GSMF, model Sat2Cen is strongly disfavored. Models KeepSat, Sat2ICL, and Sat2Cen+ICL fair far better. In fact, based on current observations, all of these models appear more or less equally viable (their relative viability depends on what one assumes about the observationally allowed range in ΔM_{-4}). We now turn to comparisons of the models with observations of BCGs and the ICL, in the hope of more strongly distinguishing between them.

4.2. *BCG Luminosities at $z \sim 0$*

We now confront our models with observations of cluster properties at $z \sim 0$. Lin & Mohr (2004) have computed virial masses from *X*-ray observations and, using the 2MASS database, estimated BCG luminosities[5] for 93 clusters at $z < 0.1$. Figure 3 plots the *K*-band BCG luminosity versus cluster virial mass for the data from Lin & Mohr (2004; *filled circles*) and for the models.[6] Several trends are apparent. Models KeepSat and Sat2ICL predict identical BCG luminosities (since in both models the central galaxy, which is identified as the BCG, does not accrete any satellite stars since $z = 1$) and are in good agreement with the observations. Model Sat2Cen is, again, in strong disagreement with the observations. Finally, the predictions of model Sat2Cen+ICL are in between those of models KeepSat and Sat2ICL and model Sat2Cen, by construction, and are mildly disfavored by the observations.

The failure of model Sat2Cen is of course no surprise in light of the results in § 4.1. The failure is, as in § 4.2, simply a manifestation of the fact that the massive end of the halo mass function

[5] Note that $\sim$70% of the BCGs in this sample are centered in the cluster to within 5% of the virial radius; in what follows we assume that all BCGs in this sample are the central galaxy.

[6] For this comparison, we have converted our halo mass definition of 334 times the mean density of the universe to the definition used in Lin & Mohr (2004), 200 times the critical density, by using an NFW density profile with a mass-dependent concentration.

in a ΛCDM cosmology evolves much more strongly from $z = 1$ to $z = 0$ than the observed evolution in the GSMF. This is corroborated by observational constraints on halo masses at various epochs which indicate that while the stellar and dark matter components grow in lockstep for lower mass systems (Heymans et al. 2006; Conroy et al. 2007), the stellar mass growth of central galaxies in high-mass halos appears to be outpaced by the growth in their halo mass at $z < 1$ (Conroy et al. 2007).

Comparison to BCG luminosities does, however, provide stronger constraints on model Sat2Cen+ICL compared to the constraints from evolution in the GSMF. Specifically, the disagreement between observations apparent in Figure 3 suggests that fewer than half of the stars from disrupted subhalos can end up in the central BCG. And indeed, from the agreement between observations and models KeepSat and Sat2ICL, we conclude that no growth is favored.

4.3. *The ICL Component at $z \sim 0$*

We now confront our models with observations of the ICL component. The notion of intracluster light arose from the observation that the extended profiles of BCGs were in excess of de Vaucouleurs profiles (Matthews et al. 1964; Schombert 1988). There is currently no strong consensus on whether the ICL is simply the outer component of the BCG or whether it is dynamically distinct. Observationally, the ICL is often defined as the total light beyond a particular surface brightness level, although recently there have been attempts to model the entire surface brightness profile with multiple components, thus separating the BCG and ICL in a less arbitrary way. For our purposes we use the data from Gonzalez et al. (2005, 2007), who have measured the surface brightness profiles for 24 BCGs at $z < 0.12$ in the *I*-band and have also measured virial masses for the clusters.

When considering the ICL, the most straightforward observable to confront with models is the combined BCG and ICL light. For this quantity one does not need to rely on the potentially arbitrary distinction between BCG and ICL. The top panel of Figure 4 plots the absolute *I*-band magnitude for the combined BCG and ICL components, $M_{\rm BCG+ICL}$, as a function of cluster virial mass,[7] for the data from Gonzalez et al. (2005; *filled circles*) and for our models. Models Sat2Cen, Sat2ICL, and Sat2Cen+ICL predict the same $M_{\rm BCG+ICL}$, since these models differ only in the way in which the stars are distributed between the BCG and ICL. As can be seen from the figure, these three models all adequately reproduce the observations over a range of cluster masses.

Model KeepSat, however, predicts a substantially different $M_{\rm BCG+ICL}$, since in this model no stars are added to the ICL nor BCG since $z = 1$. In particular, model KeepSat predicts $M_{\rm BCG+ICL} > 1$ mag lower than observations, which corresponds to a factor >2.5 lower luminosity, and because of our adopted constant mass-to-light ratio, this corresponds to the same factor lower in stellar mass. This discrepancy is far too great to be accounted for by the small effects neglected in these models, such as star formation, tidal stripping, and ICL generation at $z > 1$ (see below). Hence, observations of $M_{\rm BCG+ICL}$ strongly suggest that model KeepSat is unrealistic.

A more uncertain, but potentially more discriminating observable, is the fraction of BCG and ICL light that is in the ICL. In this case comparison between models and data must be treated carefully because the separation between ICL and BCG is not handled in the same way for different data sets. Our operational definition

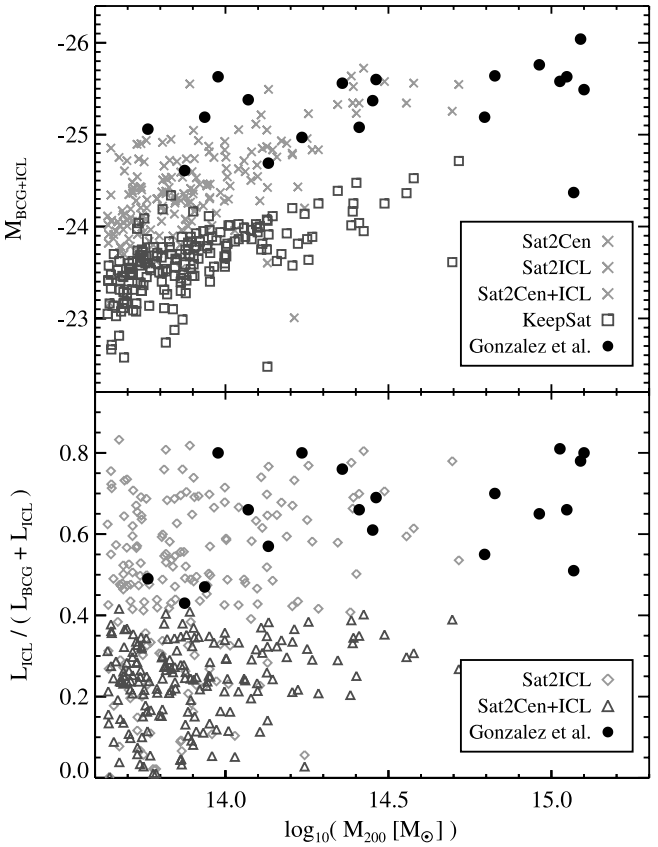

FIG. 4.— *Top panel:* Absolute *I*-band magnitudes of the combined BCG and ICL components as a function of total cluster mass. Observations at $z \sim 0$ (Gonzalez et al. 2005, 2007; *filled circles*) are compared to models KeepSat (*squares*), Sat2Cen, Sat2ICL, and Sat2Cen+ICL (*crosses*). *Bottom panel:* Fraction of BCG+ICL luminosity that is contained in the ICL component as a function of cluster virial mass, comparing observations to models Sat2ICL (*diamonds*) and Sat2Cen+ICL (*triangles*). Models Sat2Cen and KeepSat produce no ICL component. [*See the electronic edition of the Journal for a color version of this figure.*]

of ICL is simply the light not counted as the BCG by Lin & Mohr (2004). Their definition of BCG luminosity corresponds to the light within a surface brightness of $\mu_K \approx 21$ mag arcsec^{-2}. Assuming $I - K = 2$, which is appropriate for bright red galaxies, implies a separation between ICL and BCG at $\mu_I = 23$ mag arcsec^{-2}. The observational results from Gonzalez et al. (2005) which are in the *I*-band, have been recast in this way to afford the most robust comparison to our model (A. Gonzalez 2006, private communication).

The bottom panel of Figure 4 plots the ICL fraction for models Sat2ICL and Sat2Cen+ICL (recall that models Sat2Cen and KeepSat do not have an ICL component) and compares to the results from Gonzalez et al. (2005; *filled circles*). It is clear that model Sat2ICL predicts much more ICL light than the other models and an ICL light fraction that is in excellent agreement with the observations.

There are two additional routes by which the ICL can be built up that have been neglected thus far: build up of the ICL at $z > 1$ and the tidal stripping of satellites as they orbit within the cluster potential. Specifically, hydrodynamical simulations have found that ~85% of the stars in the ICL at $z = 0$ were deposited at $z < 1$ (Willman et al. 2004; Murante et al. 2007), and less than 30% of the ICL was built up by tidal stripping of satellite galaxies (Murante et al. 2007). The majority of the ICL is thus built during violent merging events with the central galaxy and/or the complete disruption of satellites—i.e., the two processes that are captured in

[7] Their definition of virial mass is the mass enclosing a region with mean density equal to 500 times the critical density; we have converted both their masses and our to a definition of 200 times the critical density; see § 4.2 for details.

our treatment of the ICL. Recent observations of the color of the ICL support the picture that stars comprising the ICL formed at $z > 1$ (Krick et al. 2006). While both processes will increase the ICL component, neither will produce enough additional ICL to account for the discrepancy between models Sat2Cen, KeepSat, and Sat2Cen+ICL and observations depicted in Figure 4—if these simulations are accurately capturing the build-up of the ICL.

One further point of clarification needs to be mentioned in this (or any) discussion of ICL. Our model and the data to which we have compared is focused on ICL surrounding the central BCG, leaving the issue of noncentral ICL (i.e., ICL associated with satellite galaxies) unaddressed. Indeed, recent observations of the Virgo Cluster indicate that there is significant amounts of ICL surrounding several satellite galaxies (Mihos et al. 2005), suggesting that noncentral ICL could be ubiquitous. In the context of our model, the ICL surrounding these satellites would have been built up from mergers *before the satellite was accreted*. Whatever the origin of the noncentral ICL, its existence does not impact the comparison between model and data presented herein.

4.4. *Implications for Star Formation Since $z = 1$*

Until now we have focused on observations that can be described with purely dissipationless modeling. Now that we have identified a dissipationless model that adequately reproduces various observations (model Sat2ICL), we can ask what more must be added to such a model in order to reproduce the observed global galaxy population. Clearly, the most important process neglected thus far is star formation, which becomes increasingly important in lower mass halos. We now turn to a discussion of the importance of star formation as a function of halo mass since $z = 1$.

We first construct a simple model that places the "true" $z = 0$ stellar mass in dark matter halos. This is accomplished using the methodology outlined in § 3, now matching the $z = 0$ GSMF to the $z = 0$ halo mass function. Such a model will have the correct $z = 0$ GSMF by construction and should have approximately the correct relation between stellar mass and halo mass since this method has been shown to reproduce numerous observations remarkably well (see § 3 for details).

Figure 5 compares these true stellar masses to stellar masses from models Sat2Cen, Sat2ICL and Sat2Cen+ICL as a function of $z = 0$ halo mass (*top panel*) and stellar mass (*bottom panel*). As before, we generate 200 realizations of these models by sampling the $z = 1$ GSMF uncertainties (recall that in these models the $z = 0$ stellar masses are products of the $z = 1$ GSMF combined with the dark matter halo merger trees to $z = 0$). The resulting mean and 1 σ dispersions are included in this figure. At large masses, the stellar masses from models Sat2ICL and Sat2Cen+ICL match the "true" stellar masses while model Sat2Cen overpredicts the true stellar masses, although all are consistent with the true masses at roughly the 2 σ level. This is not surprising, both in light of the results from previous sections and more generally because massive galaxies (which reside in massive halos) are observed to have finished forming stars by $z \approx 2$. In fact, if there is truly zero star formation in these massive galaxies since $z = 1$, then Figure 5 suggests that the $z = 0$ "true" stellar masses are best reproduced by a model in between models Sat2ICL and Sat2Cen+ICL, i.e., subhalos transfer perhaps ~80% of their stars to the ICL, and ~20% to the central galaxy. A distinction this refined should, of course, be treated with caution.

The behavior at lower masses is more interesting. In this regime the stellar masses from models Sat2Cen, Sat2ICL and Sat2Cen+ICL are substantially less than the true masses, indicating that the $z < 1$ star formation is increasingly important in halos of lower mass.

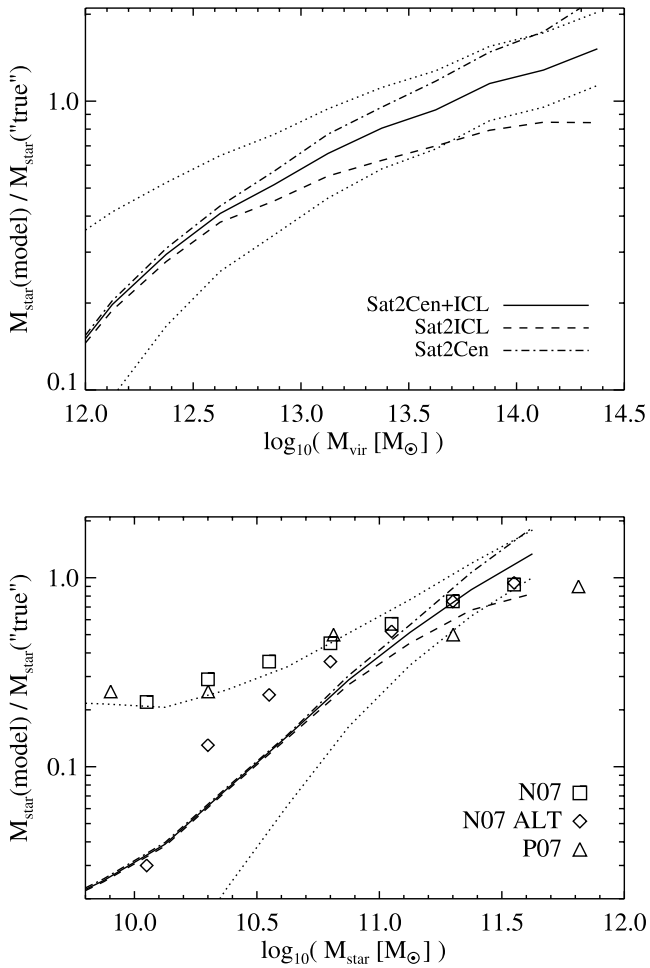

FIG. 5.—Ratio of the $z = 0$ stellar masses predicted by models Sat2Cen, Sat2ICL, and Sat2Cen+ICL to the "true" stellar masses, as a function of $z = 0$ host halo mass (*top panel*) and stellar mass (*bottom panel*). These "true" stellar masses are obtained by matching the observed $z = 0$ GSMF to the $z = 0$ halo mass function (see the text for details). Dotted lines denote the 1 σ dispersion around model Sat2Cen+ICL estimated from 200 Monte Carlo realizations that incorporate the $z = 1$ GSMF uncertainties (the dispersion around the other models is similar). The bottom panel includes observational estimates from N07 and P07); see the text for details. [*See the electronic edition of the Journal for a color version of this figure.*]

In fact, according to these models roughly 40% of the stars in $z = 0$ halos of mass $M_{\rm vir} \sim 10^{13}\ h^{-1}\ M_{\odot}$ formed at $z < 1$, while in halos of mass $M_{\rm vir} \sim 10^{12}\ h^{-1}\ M_{\odot}$~80% of the stars were formed over the same interval. Note that the models converge at lower masses, and thus these conclusions are insensitive to the way in which disrupted subhalos are handled.

The implied stellar mass growth from these models is qualitatively consistent with observed trends. Figure 5 (*bottom panel*) includes measurements from Noeske et al. (2007, hereafter N07) and Panter et al. (2007, hereafter P07). N07 measure stellar masses and star formation rates over the redshift interval $0 < z < 1$ for galaxies in the AEGIS survey (Davis et al. 2007) while P07 derive stellar masses and star formation histories for galaxies at $z \sim 0$ in the SDSS survey (Adelman-McCarthy et al. 2006). The symbols labeled "N07 ALT" are derived from average star formation histories that are slightly different than those presented in N07 but which fit the data equally well (K. Noeske 2006, private communication).

The stellar mass growth deduced from the models is somewhat high at low masses compared to the observations (although consistent within 1 σ), and may point toward an underestimate of

the stellar mass in less luminous galaxies at $z \sim 1$ (see, e.g., Nagamine et al. 2006 for a discussion of this issue).

4.5. *Caveats and Assumptions*

4.5.1. *Definition of the BCG*

It has recently come to light that standard photometry in large galaxy surveys systematically underestimates BCG luminosities for several different reasons (Lauer et al. 2007; Bernardi et al. 2007). This issue is complicated by the somewhat arbitrary distinction between BCG and ICL, as one needs a well defined notion of a BCG in order to claim that standard techniques are "missing" BCG light. The effect can be as large as 1 mag, although in such cases it appears that the ICL is included as part of the BCG. Our results are robust against these effects because our notion of a BCG is precisely that measured by the data to which we compare (i.e., by Lin & Mohr 2004), while the ICL is simply light outside the optical radius (i.e., outside the region counted as the BCG). Unfortunately, this means that our results which rely on the separation between the BCG and ICL are not directly exportable to other observations of the BCG and ICL if such observations separate these two observables in different ways. As mentioned previously, a more robust approach to this type of modeling would be to present actual surface brightness *profiles*, which could then be compared to any well-defined observational sample (see, e.g., Rudick et al. 2006).

4.5.2. *Scatter in the Galaxy-Halo Connection*

We now explore the impact of scatter in the $M_{\rm star}$-$M_{\rm vir}$ relation on our results (recall that the relation between stellar mass and halo mass utilized in the previous section was generated by assuming a one-to-one correspondence).[8] In order to explore the maximal effect that scatter can have on our results, we generate a rather extreme prescription of scatter. The scatter is included by multiplying each halo mass by a random number drawn from a Gaussian with $\sigma = 0.6$ dex (see Tasitsiomi et al. 2004 for a different prescription of scatter). Stellar masses are then matched to this random number in the standard way.[9] Figure 6 compares this model (*filled symbols*) to our standard one-to-one correspondence (*solid line*). This figure includes both distinct halos and subhalos; for the latter we use the virial mass at the epoch of accretion, as before. In addition, we include lines that indicate the amount of stellar mass a galaxy would have if its halo contained the cosmic mean baryon-to–dark matter ratio, $f_b = 0.17$, and it converted a fraction η of those baryons into stars (η is often called the star formation efficiency).

Comparison between the scatter prescription and the lines of constant star formation efficiency indicate why this prescription is extreme—there are galaxies which have $\eta \sim 1$ and indeed some rare cases where the baryon fraction in the halo exceeds f_b. At $z \sim 0$ the star formation efficiency is almost certainly $\eta < 0.25$ (Mandelbaum et al. 2006 and decreases for increasing halo mass), so we have effectively scattered galaxies, at a fixed stellar mass, to halo masses that violate, or almost violate constraints on both η and f_b. Note that this type of scatter (scattering down in halo mass at a fixed stellar mass) will likely cause the most change in the observables discussed in the previous sections because massive galaxies in less massive halos will have less violent accretion histories since $z = 1$ compared to more massive halos.

[8] Note that for our comparisons to observed luminosities the scatter in the $M_{\rm star}$-$M_{\rm vir}$ relation can be interpreted, at least in part, as scatter in M/L.

[9] If ζ denotes the halo mass multiplied by a random number drawn from a Gaussian, then the stellar masses are assigned via $n_g(>M_{{\rm star},i}) = nh(>\zeta_i)$; see eq. (1).

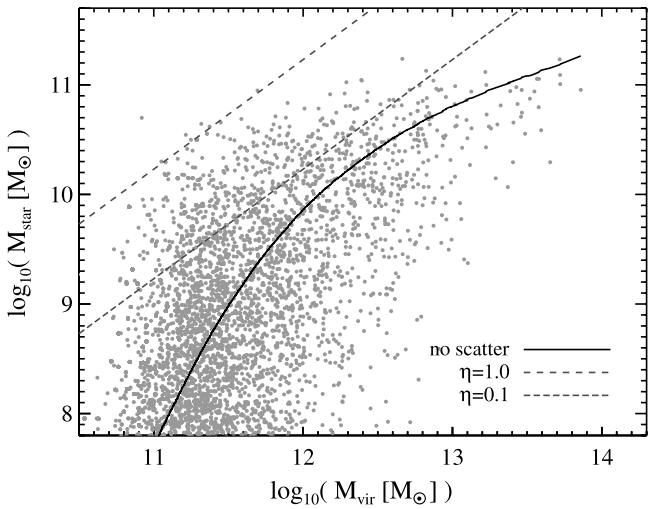

FIG. 6.—Stellar mass as a function of virial mass at $z = 1$. The solid line indicates our standard one-to-one correspondence between halo and stellar mass, while the symbols represent a prescription for scatter between the two quantities (only 25% of the total number of objects are plotted for clarity). The dashed and dot-dashed lines represent the stellar mass that a galaxy would have if it had a star formation efficiency of $\eta = 1.0$ and 0.1, respectively (assuming that the baryon-to–dark matter ratio in each halo is the cosmic mean value of 0.17). See the text for details. [*See the electronic edition of the Journal for a color version of this figure.*]

However, even with this large amount of scatter, our results remain qualitatively unchanged, although our conclusions are not as strong. For example, the model predictions for the $L_{\rm BCG}$-$M_{\rm vir}$ relation are lower by $\sim$0.1 dex, with a more pronounced tail toward lower $L_{\rm BCG}$ at lower masses. Evolution in the GSMF is also less by about the same amount. The BCG+ICL luminosity-mass relation still rules out model KeepSat, and the ICL fraction still favors model Sat2ICL.

4.5.3. *Observational Uncertainties*

In § 4.1 we explored the sensitivity of the model predictions to the adopted $z \sim 1$ GSMF; we now do the same for the BCG–cluster mass relation presented in § 4.2. We have checked by eye the BCG–cluster mass relation produced from model Sat2Cen for the 200 realizations of the $z \sim 1$ GSMF and compared them to the observations of Lin & Mohr (2004). Model Sat2Cen matches the observations approximately $\sim$13% of the time (note that this fraction is the same fraction of realizations of model Sat2Cen that match the observational constraints on evolution in the GSMF; see § 4.1). In these cases either M_* or ϕ_* (or both) are >1 σ below the mean GSMF Schechter parameters. Recall that these uncertainties are rough combined systematic and statistical uncertainties and are thus likely upper bounds. Further, the GSMF we adopt from Fontana et al. (2006) is a lower bound with respect to other observations at $z \sim 1$ (see Fig. 1). Nevertheless, any future revision of the GSMF downward by $\gtrsim 1\,\sigma$ (systematic + statistical) would weaken the constraints on the models significantly. Clearly, our results and conclusions could be sharpened with more accurate measurements of the GSMF in the future.

4.5.4. *Effects of Cosmology*

In our simulations of the ΛCDM cosmology, the adopted normalization of the power spectrum, $\sigma_8 = 0.9$, was somewhat higher than recent constraints from the 3 year *WMAP* data: $\sigma_8 \approx 0.75$–0.8 (Spergel et al. 2007). A lower value of σ_8 would imply that the same observed galaxy number density (and stellar mass) corresponds to smaller halo circular velocity and virial mass. There would also be more evolution in the abundance of massive halos

between $z = 1$ and $z = 0$, as halo formation times would be shifted to more recent time. This would imply that the amount of evolution would be larger and our conclusions would be stronger in a lower σ_8 universe. However, later formation times also imply that there would be less time for accreting halos to merge and contribute to the growth of the BCG stellar mass. The relative importance of these competing effects will have to be quantified in a future analysis similar to the one presented here with simulations of lower σ_8.

5. DISCUSSION

5.1. *Implications*

We have explored four models for the dissipationless evolution of galaxies since $z = 1$. These models were constructed to match the galaxy stellar mass function (GSMF) at $z = 1$ and differ only in the fate of satellite galaxies when the subhalo, within which the satellite is embedded, is disrupted. On confronting these models with various observations we have found that only a model in which a significant fraction of stars ($\gtrsim$80%) from disrupted subhalos are transferred to the ICL (referred to as model Sat2ICL above) is consistent with data. The failure of the other models provides significant insight into the dissipationless evolution of galaxies.

A model in which all the stars from disrupted subhalos are transferred to the central galaxy (model Sat2Cen) is strongly ruled out both by observations of the evolution in the GSMF and observations of the $z = 0 L_{\rm BCG}$-$M_{\rm vir}$ relation. Such a model would only be viable if the observed GSMF at $z \sim 1$ were significantly revised downward from the current lowest reported measurements. The failure of such a model implies that, if stars from disrupted subhalos are transferred to the central galaxy, then they cannot be put in the central regions where BCG luminosities are measured. Such a conclusion is corroborated by simulations of dissipationless (''dry'') galaxy-galaxy mergers, which find that the resulting galaxy generally becomes more extended rather than substantially brighter at the center (e.g., Boylan-Kolchin & Ma 2007; Ciotti et al. 2007 although this conclusion depends on the orbital parameters of the accreted satellite).

We have also explored an extreme model where satellites never disrupt even when their subhalos do (model KeepSat). This model fails dramatically when compared to observations of the combined luminosity of the BCG and ICL, under the assumption that the ICL is built up predominantly at $z < 1$. Although this assumption appears justified in light of recent hydrodynamical simulations, one should note that our conclusion as regards model KeepSat relies on this assumption. In our models the massive subhalos correspond to massive satellites and it is the fate of these massive satellites that most strongly affects the comparison to observations of the combined luminosities of the BCG and ICL. The failure of this model thus strongly suggests that the disruption of subhalos in our high-resolution *N*-body simulations corresponds to the disruption of satellite galaxies, at least for the most massive subhalos. This need not have been the case; recent semianalytic models (SAMs) have decoupled the dynamical evolution of subhalos from satellites when the subhalo disrupts (Croton et al. 2006; Wang et al. 2006), and hence these models produce a significant population of satellites with no identifiable subhalo (the so-called orphan population).

The failure of model KeepSat strongly suggests that in fact satellites disrupt when their subhalo disrupts, at least for massive satellites, and hence any model (including the SAMs mentioned above) which fails to tie the fates of massive satellites to their subhalos will likely fail to reproduce the observed combined luminosities of the BCG and ICL. Moreover, the failure of model KeepSat provides additional justification for previous modeling where a one-to-one relation between galaxies and halos extracted from *N*-body simulations has been assumed (e.g., Kravtsov et al. 2004; Tasitsiomi et al. 2004; Conroy et al. 2006).

The data instead favor models where most, if not all, of the stars from disrupted satellites are deposited into the ICL. Model Sat2ICL puts all stars from disrupted satellites into the ICL while model Sat2Cen+ICL puts only half into the ICL and the rest onto the BCG. Although comparisons with various observations favor model Sat2ICL, the uncertainties and assumptions discussed in previous sections suggest that reality may lie somewhere in between these two models. The strongest discriminant between these scenarios is the fraction of BCG+ICL light contained in the ICL; as elsewhere, model Sat2ICL most faithfully reproduces these observations.

There is a growing consensus that massive red galaxies were more or less in place by $z \sim 1$ (e.g., Wake et al. 2006; Cimatti et al. 2006; Bundy et al. 2006). At first glance it appears difficult to reconcile this fact with ΛCDM simulations which show that massive dark matter halos (the very halos in which these massive galaxies likely reside) grow by factors of $\gtrsim$3 since $z = 1$. The success of model Sat2ICL resolves this tension by ''hiding'' the accreted stars in the ICL. Observations of the evolution of the ICL at $z < 1$ will be needed to substantiate this picture.

The success of model Sat2ICL provides us with further insight into the nature of the ICL. Observationally, the ICL appears to have colors consistent with the BCG and thus contains primarily old stars formed at $z > 1$ (Krick et al. 2006; Gonzalez et al. 2000; Zibetti et al. 2005). Is this consistent with model Sat2ICL, where the ICL is built up by mergers with the BCG at $z < 1$? The answer to this question is most likely yes, because the subhalos that are disrupting at $z < 1$ were accreted onto the host halo at $z \sim 1$ (the average accretion epoch, weighted by the fraction of stellar mass brought in by the subhalo is 0.93). In other words, the galaxies that are contributing stars to the ICL at late times were part of the main halo at $z \sim 1$ and hence could reasonably have had their star formation truncated by one or more cluster-specific processes (e.g., ram pressure stripping or harassment) by $z \sim 1$. Thus these galaxies would be adding primarily old red stars to the ICL when they disrupt.

We mention briefly the applicability of this model to lower masses and earlier epochs. One may be concerned that scattering such a large fraction of merged galaxies into the ICL would produce too much ICL in lower mass systems like the Milky Way, where the ICL fraction is at the percent level (see Purcell et al. 2007 for a summary of the observations). However, as discussed in depth in Purcell et al. (2007), a model like the one favored herein does not produce copious amounts of ICL in lower mass systems because of the increasing virial-to-stellar mass ratio in lower mass systems. In essence, although the accretion spectrum of dark matter halos is roughly self-similar, accreted halos in lower mass systems contain relatively much fewer stars, and they thus have very little impact on the total stellar mass budget, whether scattered into the ICL or not. This is demonstrated explicitly in Purcell et al. (2007), where their model (which assumes that all stars from disrupted subhalos scatter into the ICL) produces an ICL fraction that declines from $\sim$80% in massive clusters to $\sim$1% in Milky Way–type systems, in agreement with observations.

At higher redshifts the situation is much more complex. Although we have not tested our model at earlier epochs, it is likely that this model would begin to produce too much ICL and too little galaxy light at the present day if the fraction of scattered stars was >80% at all epochs. A more detailed discussion is

deferred for later work; we simply note here that caution should be taken when extrapolating this model naively to earlier epochs.

There are several other observables which can provide additional tests of these models. Specifically, the number of galaxies, $N(M)$, and the total cluster luminosity, $L_{\rm tot}(M)$, both a function of cluster virial mass, provide independent constraints compared to the observations explored herein. However, these two observables are much more sensitive to star formation since $z = 1$ (because they include lower mass galaxies), which has been neglected in these models. Hence in the present work we have not included a comparison to these observables because such a comparison would require additional, less constrained assumptions.

5.2. *Comparison to Related Work*

Semianalytic models governing the formation and evolution of galaxies have proven capable of reproducing both strong and mild evolution of massive galaxies since $z = 1$. The models of Kitzbichler & White (2007, hereafter KW07) and Bower et al. (2006) produce relatively mild evolution in the massive end of the GSMF, although KW07 appear to overpredict the abundance of massive galaxies at $z = 0$. Meanwhile, De Lucia & Blaizot (2007) and De Lucia et al. (2006) use a semianalytic model very similar to that used in KW07 and found that massive galaxies roughly double in stellar mass since $z = 1$. This doubling in stellar mass does not strongly affect the evolution in the GSMF presented in KW07 because these authors assume 0.25 dex uncertainty in the observed stellar mass estimates at $z > 0$. This assumed uncertainty, which is likely an upper bound, increases the model GSMF at the massive end for $z > 0$, and hence masks the stronger intrinsic evolution in the model. None of these models attempt to model the ICL, and all are quite sensitive to their treatment of the merging of satellite galaxies (the various possible treatments are not explored in these models) as well as an array of model parameters. For these reasons it is difficult to draw general conclusions from these models.

Our approach most closely parallels that of Monaco et al. (2006), who used a semianalytic model to follow the evolution of the GSMF. These authors artificially turned off their star formation prescription in order to follow the dissipationless growth of galaxies since $z = 1$, similar to what we do here. When a satellite merges with a central galaxy, they transfer a fraction, $f_{\rm scatter}$, of the satellites stars to the ICL. They found that $f_{\rm scatter} \geq 0.3$ resulted in evolution in the GSMF in agreement with observations.

Several models presented in the present work are closely related to the scheme employed in Monaco et al. (2006). In particular, our models Sat2Cen, Sat2Cen+ICL, and Sat2ICL are similar to their model with $f_{\rm scatter} = 0.0$, 0.5 and 1.0, respectively.[10] In § 4.1 we showed that models Sat2Cen+ICL and Sat2ICL were indeed in agreement with the observed evolution of the GSMF while model Sat2Cen was not, similar to the conclusions of Monaco et al. (2006). However, in §§ 4.2 and 4.3 we showed that model Sat2Cen+ICL overproduced BCG luminosities at $z = 0$ and underproduced the fraction of combined BCG and ICL light contained in the ICL, while model Sat2ICL successfully reproduced both of these observations. We hence expect that the model presented in Monaco et al. (2006) would reproduce these latter two observations only if they used $f_{\rm scatter} \sim 1$. Comparing models to BCG luminosities and ICL fractions vs. cluster virial mass provides unique constraints relative to evolution in the GSMF because these two observables directly probe the properties of the most massive systems, while the high-mass end of the GSMF is sensitive to Poisson uncertainty and cosmic variance.

Each of the models presented herein make predictions for the disruption rate of satellite galaxies. White et al. (2007) used the redshift-dependent clustering of galaxies from $z \simeq 0.9$ to $z \simeq 0.5$ to constrain the disruption rate of satellite galaxies. Over this time interval, these authors found that at least 1–2 satellites brighter than $\gtrsim 1.6L_*$ per massive halo were disrupted. When focusing on satellites comparable to those in White et al., we find on average 1.1 satellites within massive halos have disrupted between $z = 1$ and $z = 0.5$ (for models other than model KeepSat, since in that model satellites never disrupt). Agreement between these results provides a satisfying cross-check for both approaches. On the one hand, we follow directly the evolution of subhalos in simulations and hence have useful information regarding their disruption. Conversely, White et al. rely primarily on evolution of the observed clustering of galaxies to constrain the disruption rate, and hence make no assumptions regarding the relation between subhalos and satellites. When combined, these results provide further weight to the idea that, over the mass ranges explored herein, disrupted subhalos correspond to disrupted satellite galaxies.

6. SUMMARY

In this paper we investigated models for the dissipationless buildup of massive central galaxies and the intracluster light, in the context of merging histories for dark matter halos in high-resolution simulations of the currently favored ΛCDM model. We used a simple model for associating galaxies with dark matter halos and subhalos at $z = 1$, using the observed galaxy stellar mass function and the mass function for halos and subhalos measured in simulations. The dissipationless evolution of galaxies in this model was tracked with the merging history of the dark matter halos extracted from simulations. We then confronted this model with data on the evolution of the galaxy stellar mass function and with the amount and fraction of cluster light that is in brightest cluster galaxies (BCGs) and in the ICL at $z = 0$, investigating where the predictions from variations in the fate of stars in merging galaxies could be distinguished.

We found that our model accurately reproduces a variety of observed properties at $z = 0$ if disrupted subhalos deposit most of their stars into the intracluster light (ICL). Other scenarios, either those in which most of the stars are deposited onto the central BCG or in which stars from disrupted halos are left behind as satellite galaxies, are strongly disfavored by the data. Such a scenario suggests that, while BCGs do not appear to evolve strongly at $z < 1$, the ICL surrounding such galaxies is growing substantially over this epoch. This scenario is corroborated by high-resolution dissipationless simulations of galaxy-galaxy mergers (Boylan-Kolchin & Ma 2007), which find that disrupted satellites preferentially build-up the outer envelope of massive galaxies.

Although ideally one should distinguish between light bound to galaxies and light that is dynamically bound only to the main halo, it is worth noting that our analysis does not explicitly distinguish between the outer parts of bright or cD galaxies and the ICL. For the purposes of this work "BCG" refers to that part of the central galaxy's light that is captured in standard survey photometry, operationally defined for most of the comparisons herein as light above a surface brightness cut of $\mu_i \approx 23$ mag arcsec^{-2}, while "ICL" refers to the light centered on the BCG but fainter than the above surface brightness cut. Further work both on the theoretical and observation side is needed to refine this distinction, and care should be taken when comparing various studies, as there is a wide variation in choices made for these definitions.

[10] Note that in their model 10% of the stars in the ICL came from the tidal stripping of satellite galaxies—a process that we have ignored in the present work.

We emphasize that models for the formation and evolution of galaxies must be seriously confronted with observations of the ICL, in addition to more conventional observations such as the GSMF and the two-point correlation function. The ICL contains a significant, if still somewhat uncertain, amount of stellar mass, and models that ignore this component will either place too much stellar mass in resolved galaxies or will fail to produce enough stars globally.

The success of this simple model lends weight to earlier implications from clustering statistics that the resolution of the current generation of *N*-body simulations is sufficient to resolve the bulk of subhalos that correspond to observed satellite galaxies in clusters. Such a confirmation unleashes an exciting array of possibilities for understanding the connection between galaxies and dark matter halos.

We thank Yen-Ting Lin, Anthony Gonzalez, Kai Noeske, and Raul Jimenez for providing their data in electronic format and for help in its interpretation, Brant Robertson for pointing out the issue of stellar mass loss, Jeremy Tinker for providing the virial mass definition conversions, and Mike Boylan-Kolchin for stimulating discussions regarding the ICL. We additionally thank Zheng Zheng, Frank van den Bosch, Michael Brown, and Martin White for helpful comments on an earlier draft, and the referee Pierluigi Monaco for comments that improved the quality of the manuscript. C. C. thanks the city of Montreal for its unrelenting hospitality during the early stages of this work.

The simulations were run on the Columbia machine at NASA Ames and on the Seaborg machine at NERSC (Project PI: Joel Primack). We would like to thank Anatoly Klypin for running these simulations and making them available to us. We are also indebted to Brandon Allgood for providing the merger trees. A. V. K. is supported by the National Science Foundation (NSF) under grants AST 02-39759 and AST 05-07666, by NASA through grant NAG5-13274, and by the Kavli Institute for Cosmological Physics at the University of Chicago. This work made extensive use of the NASA Astrophysics Data System and of the astro-ph preprint archive at http://arxiv.org.

REFERENCES

Adelman-McCarthy, J. K., et al. 2006, ApJS, 162, 38
Allgood, B. 2005, Ph.D. thesis, Univ. California (Santa Cruz)
Andreon, S. 2006, A&A, 448, 447
Baldry, I. K., Glazebrook, K., Brinkmann, J., Ivezić, Ž., Lupton, R. H., Nichol, R. C., & Szalay, A. S. 2004, ApJ, 600, 681
Baugh, C. M., Cole, S., & Frenk, C. S. 1996, MNRAS, 283, 1361
Bell, E. F., McIntosh, D. H., Katz, N., & Weinberg, M. D. 2003, ApJS, 149, 289
Bell, E. F., et al. 2006, ApJ, 640, 241
Berlind, A. A., & Weinberg, D. H. 2002, ApJ, 575, 587
Bernardi, M., Hyde, J. B., Sheth, R. K., Miller, C. J., & Nichol, R. C. 2007, AJ, 133, 1741
Berrier, J. C., Bullock, J. S., Barton, E. J., Guenther, H. D., Zentner, A. R., & Wechsler, R. H. 2006, ApJ, 652, 56
Blanton, M. R. 2006, ApJ, 648, 268
Borch, A., Meisenheimer, K., Bell, E. F., Rix, H.-W., Wolf, C., Dye, S., Kleinheinrich, M., Kovacs, Z., & Wisotzki, L. 2006, A&A, 453, 869
Bower, R. G., Benson, A. J., Malbon, R., Helly, J. C., Frenk, C. S., Baugh, C. M., Cole, S., & Lacey, C. G. 2006, MNRAS, 370, 645
Bower, R. G., Lucey, J. R., & Ellis, R. S. 1992, MNRAS, 254, 601
Boylan-Kolchin, M., & Ma, C.-P. 2007, MNRAS, 374, 1227
Brown, M. J. I., Dey, A., Jannuzi, B. T., Brand, K., Benson, A. J., Brodwin, M., Croton, D. J., & Eisenhardt, P. R. 2007, ApJ, 654, 858
Bundy, K., Ellis, R. S., & Conselice, C. J. 2005, ApJ, 625, 621
Bundy, K., et al. 2006, ApJ, 651, 120
Caputi, K. I., McLure, R. J., Dunlop, J. S., Cirasuolo, M., & Schael, A. M. 2006, MNRAS, 366, 609
Cimatti, A., Daddi, E., & Renzini, A. 2006, A&A, 453, L29
Ciotti, L., Lanzoni, B., & Volonteri, M. 2007, ApJ, 658, 65
Cirasuolo, M., et al. 2007, MNRAS, 380, 585
Cole, S., et al. 2001, MNRAS, 326, 255
Colín, P., Klypin, A. A., Kravtsov, A. V., & Khokhlov, A. M. 1999, ApJ, 523, 32
Conroy, C., Wechsler, R. H., & Kravtsov, A. V. 2006, ApJ, 647, 201
Conroy, C., et al. 2007, ApJ, 654, 153
Croton, D. J., et al. 2006, MNRAS, 365, 11
Davis, M., et al. 2007, ApJ, 660, L1
De Lucia, G., & Blaizot, J. 2007, MNRAS, 375, 2
De Lucia, G., Springel, V., White, S. D. M., Croton, D., & Kauffmann, G. 2006, MNRAS, 366, 499
Drory, N., Bender, R., Feulner, G., Hopp, U., Maraston, C., Snigula, J., & Hill, G. J. 2004, ApJ, 608, 742
Faber, S. M., et al. 2005, ApJ, submitted (astro-ph/0506044)
Fontana, A., et al. 2004, A&A, 424, 23
———. 2006, A&A, 459, 745
Gonzalez, A. H., Zabludoff, A. I., & Zaritsky, D. 2005, ApJ, 618, 195
Gonzalez, A. H., Zabludoff, A. I., Zaritsky, D., & Dalcanton, J. J. 2000, ApJ, 536, 561
Gonzalez, A. H., Zaritsky, D., & Zabludoff, A. I. 2007, ApJ, 666, 147
Heymans, C., et al. 2006, MNRAS, 371, L60
Jimenez, R., Bernardi, M., Haiman, Z., Panter, B., & Heavens, A. F. 2006, ApJ, submitted (astro-ph/0610724)
Jungwiert, B., Combes, F., & Palouš, J. 2001, A&A, 376, 85
Kitzbichler, M. G., & White, S. D. M. 2007, MNRAS, 376, 2 (KW07)
Klypin, A., Gottlöber, S., Kravtsov, A. V., & Khokhlov, A. M. 1999, ApJ, 516, 530
Kravtsov, A. V. 1999, Ph.D. thesis, New Mexico State Univ.
Kravtsov, A. V., Berlind, A. A., Wechsler, R. H., Klypin, A. A., Gottlöber, S., Allgood, B., & Primack, J. R. 2004, ApJ, 609, 35
Kravtsov, A. V., & Klypin, A. A. 1999, ApJ, 520, 437
Kravtsov, A. V., Klypin, A. A., & Khokhlov, A. M. 1997, ApJS, 111, 73
Krick, J. E., Bernstein, R. A., & Pimbblet, K. A. 2006, AJ, 131, 168
Lauer, T. R., et al. 2007, ApJ, 662, 808
Lin, Y.-T., & Mohr, J. J. 2004, ApJ, 617, 879
Mandelbaum, R., Seljak, U., Kauffmann, G., Hirata, C. M., & Brinkmann, J. 2006, MNRAS, 368, 715
Masjedi, M., et al. 2006, ApJ, 644, 54
Matthews, T. A., Morgan, W. W., & Schmidt, M. 1964, ApJ, 140, 35
Mihos, J. C., Harding, P., Feldmeier, J., & Morrison, H. 2005, ApJ, 631, L41
Monaco, P., Fontanot, F., & Taffoni, G. 2007, MNRAS, 375, 1189
Monaco, P., Murante, G., Borgani, S., & Fontanot, F. 2006, ApJ, 652, L89
Murante, G., Giovalli, M., Gerhard, O., Arnaboldi, M., Borgani, S., & Dolag, K. 2007, MNRAS, 377, 2
Murante, G., et al. 2004, ApJ, 607, L83
Naab, T., Khochfar, S., & Burkert, A. 2006, ApJ, 636, L81
Nagai, D., & Kravtsov, A. V. 2005, ApJ, 618, 557
Nagamine, K., Ostriker, J. P., Fukugita, M., & Cen, R. 2006, ApJ, 653, 881
Neistein, E., van den Bosch, F. C., & Dekel, A. 2006, MNRAS, 372, 933
Neyrinck, M. C., Hamilton, A. J. S., & Gnedin, N. Y. 2004, MNRAS, 348, 1
Noeske, K. G., et al. 2007, ApJ, 660, L47 (N07)
Pahre, M. A. 1999, ApJS, 124, 127
Panter, B., Jimenez, R., Heavens, A. F., & Charlot, S. 2007, MNRAS, 378, 1550 (P07)
Partridge, R. B., & Peebles, P. J. E. 1967, ApJ, 147, 868
Purcell, C. W., Bullock, J. S., & Zentner, A. R. 2007, ApJ, 666, 20
Rudick, C. S., Mihos, J. C., & McBride, C. 2006, ApJ, 648, 936
Schombert, J. M. 1988, ApJ, 328, 475
Seigar, M. S., Graham, A. W., & Jerjen, H. 2007, MNRAS, 378, 1575
Shankar, F., Lapi, A., Salucci, P., De Zotti, G., & Danese, L. 2006, ApJ, 643, 14
Sommer-Larsen, J., Romeo, A. D., & Portinari, L. 2005, MNRAS, 357, 478
Spergel, D. N., et al. 2007, ApJS, 170, 377
Tasitsiomi, A., Kravtsov, A. V., Wechsler, R. H., & Primack, J. R. 2004, ApJ, 614, 533
Tasitsiomi, A., Wechsler, R. H., Kravtsov, A. V., & Klypin, A. 2007, in preparation
Thomas, D., Maraston, C., Bender, R., & Mendes de Oliveira, C. 2005, ApJ, 621, 673
Trager, S. C., Faber, S. M., Worthey, G., & González, J. J. 2000, AJ, 120, 165

Vale, A., & Ostriker, J. P. 2004, MNRAS, 353, 189
———. 2006, MNRAS, 371, 1173
———. 2007, MNRAS, submitted (astro-ph/0701096)
van Dokkum, P. G. 2005, AJ, 130, 2647
van Dokkum, P. G., & Franx, M. 2001, ApJ, 553, 90
Wake, D. A., et al. 2006, MNRAS, 372, 537
Wang, L., Li, C., Kauffmann, G., & de Lucia, G. 2006, MNRAS, 371, 537
Weinberg, D. H., Colombi, S., Davé, R., & Katz, N. 2006, ApJ, submitted (astro-ph/0604393)
White, M., Zheng, Z., Brown, M. J. I., Dey, A., & Jannuzi, B. T. 2007, ApJ, 655, L69
Willman, B., Governato, F., Wadsley, J., & Quinn, T. 2004, MNRAS, 355, 159
Willmer, C. N. A., et al. 2006, ApJ, 647, 853
Zheng, Z., et al. 2005, ApJ, 633, 791
Zibetti, S., White, S. D. M., Schneider, D. P., & Brinkmann, J. 2005, MNRAS, 358, 949